



Using rare earth elements to monitor sediment sources from a miniature model of a small watershed in the Three Gorges area of China



Gang Liu^{a,b,c,*}, Hai Xiao^a, Puling Liu^a, Qiong Zhang^a, Jiaqiong Zhang^a

^a State Key Laboratory of Soil Erosion and Dryland Farming on the Loess Plateau, Institute of Soil and Water Conservation, Northwest A&F University, Yangling 712100, People's Republic of China

^b Institute of Soil and Water Conservation of Chinese Academy of Sciences and Ministry of Water Resources, Yangling 712100, People's Republic of China

^c USDA-ARS National Sedimentation Laboratory, Oxford, MS 38655, USA

ARTICLE INFO

Article history:

Received 19 February 2015

Received in revised form 12 March 2016

Accepted 31 March 2016

Available online 14 April 2016

Keywords:

Purple soil

Soil loss

Runoff

Gully erosion

Landform

ABSTRACT

Understanding soil erosion processes at different landscape positions is important in order to predict and control watershed soil losses. Rare earth elements (REEs) can be used to trace eroded soil sources but their efficacy may be soil dependent. We constructed a miniature watershed model of a small watershed located in the Three Gorges Area of China, and used oxides of eight REEs to trace the erosion of a purple soil. The miniature watershed was divided into eight regions containing a different landform type as a potential sediment source. A different REE was applied in each region. Redistributions of the REEs under three successive simulated rainfall events with intensities of 1.0, 1.5 or 2.0 mm min⁻¹ were examined. The percentage contribution from each region to the total soil loss from the watershed fluctuated relative to landform type during the three rainstorms. Contributions from the lower main gully decreased before stabilizing, while those from the upper main gully increased before decreasing, and those from other sources all increased before stabilizing. Overall, the contribution of the gully system, comprising main and branch gullies, was greater than that of the slopes. Contributions from the gully system tended to decrease with increases in rainfall intensity and rainstorm duration while those from the slopes increased. A comparison of the calculated and actual soil loss masses indicated that the accuracy of the REE tracing method was less for the coarse textured purple soil than those previously found for fine textured soils. The increased errors, likely due to the assumption used in the calculation that there is no particle size selectivity during erosion, needs to be addressed. This pilot study provided a technical reference for the use of REEs in monitoring sediment sources from a natural watershed, and a theoretical basis for soil conservation in the Three Gorges Area.

© 2016 Elsevier B.V. All rights reserved.

1. Introduction

Soil erosion has become a serious problem in the Three Gorges Area of China because of long-term poor land management and frequent heavy rainstorms. The Three Gorges Area covers 21 cities and counties in Chongqing Municipality and Hubei Province, and has a total land area of 58,800 km². Large areas of arable land are on steep slopes, which are susceptible to soil erosion. The annual soil loss in this area is estimated to be 157 million t of which 40 million t enters the Yangtze River at the rate of 700 t km⁻² year⁻¹ (Lu and Higgitt, 1998; Lu et al., 2003). The severe soil erosion has led to the loss of a non-renewable resource, pollution, sedimentation, increased flooding, and reduced food security (Shi and Shao, 2000; Anonymous, 2004; Liu et al., 2011a). Consequently, there is an urgent need to implement soil erosion

control practices in the watersheds around the Yangtze River in a way that is as cost effective as possible.

Understanding the erosion processes in field plots and small watersheds at different landscape positions is the key to developing soil erosion prediction models that can provide a scientific basis for soil and water conservation planning (Shi et al., 1997; Polyakov et al., 2004, 2009; Kimoto et al., 2006a). Conventional erosion monitoring techniques, e.g., using runoff plots and ground and stereo-photo surveys, have provided much information for the development of strategies used in soil and water conservation. However, these methods are relatively expensive and cannot provide quantitative information about all of the temporal and spatial distributions of erosion processes within a watershed (Mahler et al., 1998; Liu et al., 2004, 2011b; Li et al., 2006).

One monitoring technique involving tagging the soil with tracers has been successfully utilized in the natural sciences to study transport processes and the redistribution of various pollutants. A number of substances may be used as tracers. These substances can be classified as either occurring naturally or being introduced artificially. Tracers can be introduced into soil in two ways: (1) naturally as fallout

* Corresponding author at: Institute of Soil and Water Conservation, Northwest A&F University, No. 26, Xinong Road, Yangling, Shaanxi Province 712100, People's Republic of China.

E-mail address: gliu@foxmail.com (G. Liu).

(e.g., ^{137}Cs , ^7Be , and ^{210}Pb) (Walling and He, 1997; Wallbrink et al., 2003; Liu et al., 2011b); or (2) deliberately either by tagging soil particles with trace elements (e.g., noble metals, ^{59}Fe , ^{134}Cs , ^{60}Co) (Wooldridge, 1965; Olmez et al., 1994; Greenwood, 2012; Greenwood et al., 2014) or by incorporating trace particles into the soil body (e.g., magnetic or glass beads) (Young and Holt, 1968; Ventura et al., 2001).

Rare earth elements (REEs) are the elements with atomic numbers ranging between 57 and 71. They have similar chemical properties. The REEs are ideal for use as soil tracers because they are strongly adsorbed on soil particles without interfering in their movement. They can be readily and accurately analyzed, especially as they have low background concentrations in the soil and are chemically stable, plant uptake is low, and they are environmentally safe (Mahler et al., 1998; Zhang et al., 2001). Powdered REE oxides are industrial products that are insoluble in water and other basic solvents (Michaelides et al., 2010). They have been utilized in soil erosion research that includes studies on soil erosion processes, redistribution of eroded materials, deposition, and sedimentation (Tian et al., 1994; Matisoff et al., 2001; Zhang et al., 2003; Polyakov and Nearing, 2004; Yang et al., 2008). However, soil erosion studies have mainly concentrated on soil with high contents of clay or silt particles (Zhang et al., 2001, 2003; Polyakov and Nearing, 2004; Lei et al., 2006; Li et al., 2006; Stevens and Quinton, 2008). Most of the soils in the Three Gorges Area (e.g., purple soils) have a high content of sand particles. Different size fractions of soil particles absorb REEs to different degrees (Mahler et al., 1998; Zhang et al., 2001; Kimoto et al., 2006b). Furthermore, in the Three Gorges Area, 54.1% of the area has slopes of between 7° and 25° , and 37.5% of the area has slopes of more than 25° (Shi et al., 2009). Steeper slopes tend to induce greater size selectivity of eroded sediment and, as a result, the particle size distribution of the suspended sediment is different from that of the *in situ* soil in a watershed (Shi et al., 2012a,b,c). Thus, the potential precision of applying REEs in order to trace soil erosion in this area remains unknown.

REEs are relatively expensive. Therefore, in order to use them cost effectively, observations of how to use them in the Three Gorges area are needed. There should be some idea of where and to what level they should be distributed within a small watershed in order to study erosion processes at various sites. A possible way to address these issues is to conduct a pilot study that uses a miniature watershed model that is representative of a local small watershed and to use REEs to investigate the soil erosion occurring in the model under simulated rainstorms.

The aims of this paper were to: (1) investigate the contributions of eroded sediments from various positions in a miniature watershed during three simulated rainfall events; and (2) assess the potential of applying REEs in order to trace soil erosion in a natural watershed in the Three Gorges Area. Results from this pilot study should not only provide a technical reference for the use of REEs in monitoring sediment sources from watersheds but also a theoretical basis for the development of soil erosion prediction models and of soil and water conservation in the Three Gorges Area of China.

2. Materials and methods

2.1. Experimental setup

A field survey was conducted of a small watershed ($31^\circ 12' \text{ N}$ to $31^\circ 15' \text{ N}$, $110^\circ 40' \text{ E}$ to $110^\circ 43' \text{ E}$) located in the Wangjiaqiao watershed, Zigui County of Hubei Province, China. The watershed is approximately 50 km northwest of the Three Gorges Dam and covers an area of 0.2 ha. The climate is subtropical with mean temperatures between 11° C and 18° C . Annual precipitation averages 1016 mm, of which 70% occurs between May and September. The survey data was then used to construct a miniature replica of the watershed at a scale of 1:100 in the simulated rainfall testing grounds of the China Three Gorges University. The base and side boundaries of the miniature watershed were constructed of

bricks and concrete to match the boundaries and topography of the natural watershed. A layer of sand covering the concrete base facilitated the drainage of water. The sand was covered by a 10-cm layer of purple soil collected from the upper 20-cm layer of cultivated land in the surveyed watershed.

Purple soil forms over purple sandy shale and is classified as an Entisol according to the soil taxonomic system of the United States Department of Agriculture (Soil Survey Staff, 1999). It covers approximately 78.7% of the land in the Three Gorges Area (Shi et al., 2009). The soil had an organic matter content of 0.97% and comprised 1.97% clay ($<0.002 \text{ mm}$), 19.53% silt (0.002 mm to 0.05 mm), and 78.50% sand (0.05 mm to 2 mm) according to the US Soil Taxonomy Classification.

The following procedures were used in the placement of the purple soil layer in the miniature watershed. First, soil samples, each containing a different REE, were prepared. Eight different powdered REE oxides, which included La_2O_3 , CeO_2 , Nd_2O_3 , Sm_2O_3 , Eu_2O_3 , Tb_4O_7 , Ho_2O_3 , and Yb_2O_3 , were chosen for this study based on their price, amount to be applied, and susceptibility to detection (Liu et al., 1997). Each of the powdered oxides was evenly mixed into a separate soil sample (Liu et al., 1997). During mixing, the weighted soil was gradually added and the REE concentration was step-by-step diluted until mixed soil reached to the desired amount and concentration. The amounts and concentrations of the REE oxides used are given in Table 1. The miniature watershed was divided into 8 different landform types that were potential sediment sources, distributed across the watershed at 14 locations. The positions of the gully edge lines and section borders in the miniature watershed were then marked out with white limestone powder according to the topographic map of the surveyed watershed to ensure that geomorphologies of both watersheds were consistent. The sections were then separated from each other by pieces of sheet iron (10 cm high) to avoid cross-contamination among the soil samples containing different REEs during packing and to ensure that the surface soil layer was of uniform thickness. The purple soil samples mixed with the different REEs were then packed into the various zones according to the region designation, which is described below and illustrated in Fig. 1. Packing was carried out in 2 cm lifts to attain the desired uniform mean bulk density (1.3 g cm^{-3}) and water content (15% by weight). The pieces of sheet metal were then removed. The micro-topography of the watershed surface was then molded and smoothed, and the soil was pre-wetted to moist surface condition, covered with a plastic sheet to limit evaporation, and left for three months without disturbance to enhance the binding of the REEs to the soil particles.

Fig. 1 shows the miniature watershed, with an area of approximately 20 m^2 . The elevations of the highest and lowest positions were about 1.3 and 0.4 m, respectively. The watershed had one main gully and two branch gullies. The main gully was 5.5 m long from its highest position to the watershed outlet. The two sides of the main gully each had one branch gully. The left and right gullies were 2.2 and 1.9 m long, respectively. The general height of gully walls was 15–20 cm. The other landform information was listed in Table 1. Fig. 1 shows a region boundary line that bisects the slopes thereby dividing the regions on the lower slopes from those on the upper slopes. The upstream upper and lower slopes received La_2O_3 (REE I) and Yb_2O_3 (REE II), respectively. The downstream upper and lower slopes had CeO_2 (REE III) and Sm_2O_3 (REE IV) applied, respectively. The upper and lower parts of the main gully had Eu_2O_3 (REE V) and Tb_4O_7 (REE VI) applied, respectively. The upper and lower parts of the branch gullies had Nd_2O_3 (REE VII) and Ho_2O_3 (REE VIII) applied, respectively (Table 1). Samples of each soil-REE mixture were reserved for analysis.

2.2. Experimental procedure

A rainfall simulator with nine sets of three nozzles was positioned above the watershed at a height of 6 m. The simulator sprayed tap water (sodium adsorption ratio = 1.94, electrical conductivity =

Table 1
Parameters pertinent to the application of rare earth element (REE) oxides to an erosion study in a miniature watershed and the landform information.

Parameters	Rare earth element oxides							
	La ₂ O ₃	Yb ₂ O ₃	CeO ₂	Sm ₂ O ₃	Eu ₂ O ₃	Tb ₄ O ₇	Nd ₂ O ₃	Ho ₂ O ₃
Purity (%)	99.99	99.99	99.99	99.95	99.99	99.99	99.5	99.95
Background concentration of REEs (mg kg ⁻¹)	24.12	1.87	41.23	4.23	0.76	0.55	12.99	0.59
REE application concentration (mg kg ⁻¹)	858.6	89.2	1423.8	143.2	12.3	5.3	505.2	13.4
REE oxide application mass (g)	283.18	29.86	553.21	54.69	3.94	1.62	100.48	2.76
REE number	I	II	III	IV	V	VI	VII	VIII
Landform type	Upstream upper slopes	Upstream lower slopes	Downstream upper slopes	Downstream lower slopes	Upper main gully	Lower main gully	Upper branch gullies	Lower branch gullies
Number of zones	2	2	2	2	1	1	2	2
Relative area of each REE (%)	19.5	14.2	19.5	17.6	9.2	8.6	5.4	6.0
Average slope gradient (°)	7	9	8	9	Bottom: 15 Sides: 30	Bottom: 8 Sides: 25	Bottom: 15 Sides: 30	Bottom: 10 Sides: 25

0.87 ds m⁻¹) horizontally to simulate rainwater; raindrops then fell vertically onto the surface of the watershed after following a parabolic trajectory with a distribution uniformity greater than 86% which was determined by Christiansen coefficient (Williams et al., 1998).

Three rainstorms with intensities of 1.0, 1.5, and 2.0 mm min⁻¹ and median raindrop diameters of 2.46, 3.18, and 3.54 mm, respectively, were each simulated for 30 min. These intensities were based on the natural maximum rainfall intensity occurring for a 30-min period during moderate and heavy rainstorms in the study region. The watershed was covered with a plastic sheet after every rainfall and left undisturbed until the next rainfall, three days later. The soil was pre-wetted to moisten surface before only the first rainfall application, so the runoff developed very early in every storms. Runoff and sediments were collected, at the outlet of the watershed, in a series of plastic containers at intervals of 2 min throughout the storms. The volume of water in each container was measured, and the sediment was air dried and weighed.

2.3. Laboratory analyses

A modified standard methodology for extracting metals from environmental samples (US EPA, 1995) was used to extract the REE oxides from the various soil-REE mixtures and sediment samples in a sequence that combined ten steps. (1) A 50-g sample of the air-dried soils or sediment samples was taken and ground to pass through a 0.15-mm sieve. (2) Two 25-mg subsamples of the sieved sample were

used for the analysis of their REE contents and were considered to be replicates; the 25-mg subsample was placed in a 50-ml polytetrafluoroethylene (PTFE) cylindrical flask. (3) 0.5 ml of concentrated HNO₃ (68% by weight) and 1 ml concentrated HF (48% by weight) were added to the subsample. (4) The flask was covered by a tightly fitting lid and the flask was then sealed into a tightly fitting steel sheath before heating at 185 °C in an oven for 24 h. (5) The flask was cooled to room temperature, the lid was removed, and the open flask was then heated at 130 °C on an electric hot plate until the subsample was almost dry. (6) 1 ml of concentrated HNO₃ (68% by weight) was added and the suspension was heated as in step 5 until the sample was almost dry. (7) Steps (3), (4), (5), and (6) were repeated one more time. (8) 5 ml of HNO₃ solution was added to the flask, the lid was tightened, and the sealed flask was put into the steel sheath and heated at 130 °C in an oven for 3 h. (9) The flask was cooled to room temperature and the suspension was transferred to a 50-ml volumetric flask in which the volume was made up to 50 ml with de-ionized water (18 MΩ cm⁻¹). (10) The volumetric flask was shaken well, and the suspension was transferred to a 10-ml polyethylene centrifuge tube and centrifuged to obtain clear extracts for REE determinations. Mean values of the two subsamples (replicates) were calculated for all of the REE analyses.

Inductively Coupled Plasma Mass Spectrometry (X Series 2 ICP-MS, Thermo Fisher Scientific, US) analysis of the extracts containing REEs was carried out at the College of Chemistry and Life Science, China Three Gorges University. A stock internal standard solution containing

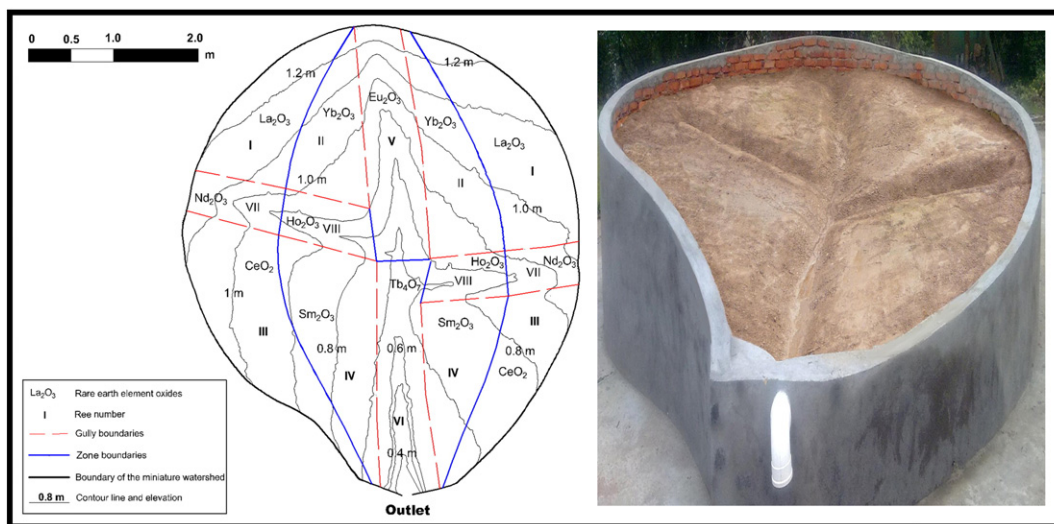


Fig. 1. Distribution of eight rare earth element oxides in 14 zones (8 landform types, REE I to VIII regions) in the miniature watershed. I, upstream upper slopes; II, upstream lower slopes; III, downstream upper slopes; IV, downstream lower slopes; V, upper main gully; VI, lower main gully; VII, upper branch gullies; VIII, lower branch gullies. Blue lines represent the division of upper and lower slope zones. Red lines represent distinction of hillslope and gully zones.

Rh and Re ($10 \mu\text{g l}^{-1}$) was added to each centrifuge tube. Three separate measurements were made for each extract and the mean value of the measurements was calculated.

The particle size distributions of the parent soils and of the sediments were measured using laser diffraction (Mastersizer 2000, Malvern Instruments, Malvern, UK). All samples were pretreated with hydrogen peroxide to remove organic matter and chemically dispersed using sodium hexametaphosphate.

2.4. Data processing

Data obtained from the chemical analyses of the soil and sediment samples were used to determine soil erosion patterns and to identify the sediment sources. The REE data were analyzed based on a comparison of the REE tracer concentrations in the sediment samples with their background and application levels. For the i th ($i = 1, 2, 3, \dots, 15$) time increment, the mass of soil loss from REE j ($j = 1, 2, 3, \dots, 8$) region and its relative proportion in the entire watershed can be calculated using Eqs. (1) and (2),

$$w_{ij} = \frac{(R_{ij} - B_j) \times W_i}{C_j} \quad (1)$$

$$r_{ij} = \frac{w_{ij}}{W_i} \quad (2)$$

where w_{ij} is the mass of soil loss from REE j region for the i th time increment (kg); R_{ij} is the actual concentration of REE j in the sediment samples for the i th time increment (mg kg^{-1}); B_j is the background concentration of REE j (mg kg^{-1}); W_i is the mass of the sediment samples from the entire watershed for the i th time increment (kg); C_j is the applied concentration of REE j (mg kg^{-1}); and r_{ij} is the relative proportion of soil loss from REE j region in the soil loss from the entire watershed for the i th time increment. Experimental error was estimated using Eq. (3):

$$\sigma = \left(\frac{\sum_{j=1}^8 w_j}{W} - 1 \right) \times 100\% \quad (3)$$

where σ is the experimental error estimated by comparing the calculated and actual masses of soil loss.

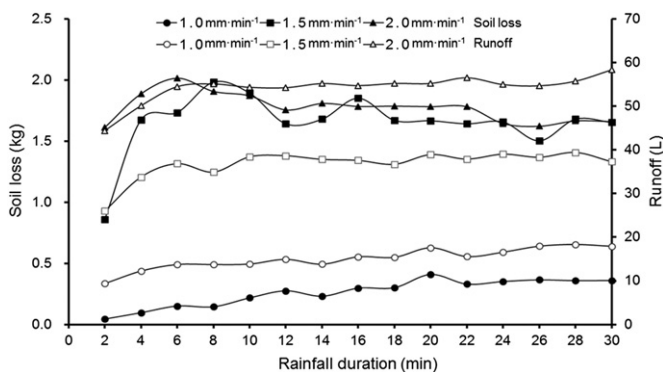


Fig. 2. Runoff and soil loss amounts from the miniature watershed as a function of rainfall duration under three successive rainstorms of different intensities.

3. Results and discussion

3.1. Temporal changes in the amounts of runoff and soil loss

Fig. 2 shows that the amount of runoff initially tended to increase relatively rapidly and then gradually stabilized during the three rainfall events. This pattern occurs because a seal formed over the soil surface during the rainstorms as a result of aggregate breakdown and compaction caused by the physical impact of raindrops and dispersion by physico-chemical processes (Agassi et al., 1981). The seal reduced soil infiltrability thereby increasing the amount of runoff (Moore and Singer, 1990). The amount of runoff gradually stabilized as the degree of seal formation reached an equilibrium value. Furthermore, higher rainfall intensities accelerated the seal formation process and the pattern thus became clearer as the rainfall intensity increased (Liu et al., 2010). Seals tended to be formed to a greater degree as rainfall intensity increased. This was indicated by the increased amounts of runoff after taking the increases due to the extra rainfall into account. It should be noted that, in this study, we used tap water to simulate rainwater, and that this likely reduced the degree of seal formation attributable to dispersion by physico-chemical processes and, hence, reduced the amount of runoff and erosion that might have occurred under deionized simulated rainfall (Agassi et al., 1981).

Although the changes in the amounts of runoff tended to follow similar patterns during all three of the rainfall events, the changes in the amounts of soil loss tended to follow different patterns (Fig. 2). The amount of soil loss under the rainfall intensity of 1.0 mm min^{-1} increased gradually until the end of the rainfall event because of the increasing shear force that scoured the soil surface due to the increasing amount of runoff (Fig. 2); this process was enhanced because the increased amounts of runoff also contained more sediments. Furthermore, the amount of soil loss only increased slowly because rills were relatively undeveloped on the slopes under this rainstorm and did not cause notable increases in erosion. Appearance of rills would increase soil loss especially during the initial development phase (Lei et al., 2006; Liu et al., 2011b).

In contrast, the amount of soil loss under the higher rainfall intensity of 1.5 mm min^{-1} increased sharply following runoff initiation. This occurred for a number of reasons. First, rills on the slopes continued to be developed during successive storms, and the increased intensity induced more rapid rill development leading to the increased overland flow and to increased erosion rates. Second, the higher runoff rates led to a rapid increase in soil erosion within the gullies from both sides and gully bottom. Third, despite being compacted, the soil is coarse-grained, disturbed and lacks cohesion to resist erosion, which can also contribute to the increasing soil loss. Finally, any loose material remaining on the soil surface after the first storm was readily washed off in the initial phases of the second storm. The amount of soil loss fluctuated with rainfall duration. This can be attributed to the discontinuous process of the collapse of rill banks on the slopes and in the gullies.

In the third storm with an intensity of 2.0 mm min^{-1} , the development of the rill and gully system was relatively stable. Hence, the increased runoff did not cause an obvious increase in soil loss. Furthermore, while there were still fluctuations in the amounts of soil loss, these were less severe in the third storm as compared with the second storm.

3.2. Amount and relative proportion of soil loss from different landform types

Under the rainfall intensity of 1.0 mm min^{-1} , soil erosion in every region tended to increase erratically. Soil erosion increased relatively rapidly and in greater amounts in REE V and VI regions, which were the main gully areas (Fig. 3a). However, the change in the contributions to the whole watershed erosion amount was different from these two regions (Fig. 4a). The contribution from the lower main gully (REE VI)

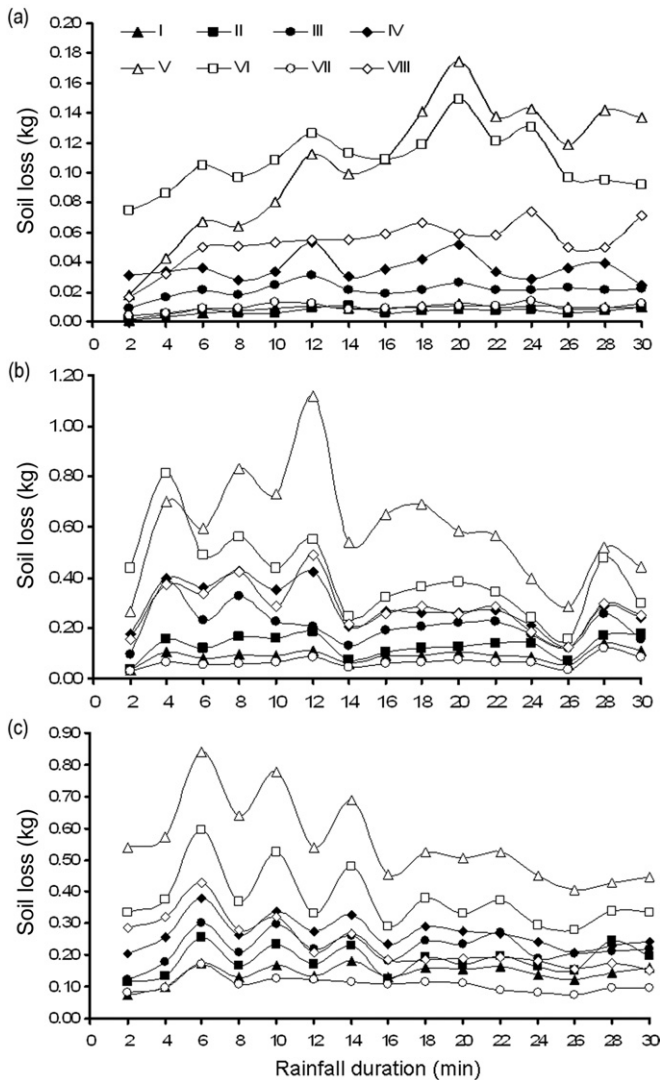


Fig. 3. Soil loss amounts from each region (REE I to VIII) of the miniature watershed as a function of rainfall duration under three successive rainstorms with different intensities: (a) 1.0 mm min^{-1} , (b) 1.5 mm min^{-1} , and (c) 2.0 mm min^{-1} . I, upstream upper slopes; II, upstream lower slopes; III, downstream upper slopes; IV, downstream lower slopes; V, upper main gully; VI, lower main gully; VII, upper branch gullies; VIII, lower branch gullies.

decreased from 48% to 24%, whereas that from the upper main gully (REE V) increased from 12% to 38%. The contributions from the other regions fluctuated within smaller ranges than those of the gullies. The contribution of main gully more than other regions to the total soil loss may be attributed to both the concentrated runoff in main gully with higher erosion capacity and being coarser soil with less cohesion supplying more material.

The amounts of soil loss from every region during the second rainstorm were notably greater than during the first rainstorm (Fig. 3b). Maximum and minimum soil losses from REE VI region per 2-minute interval during the second rainstorm were 0.813 and 0.158 kg, respectively, which were between 2.1 and 5.5 times greater than the values obtained during the first rainstorm (0.149 and 0.075 kg), which had a lower intensity. The higher amount of soil loss can be attributed in part to the higher rate of initial removal of any loose material remaining on the soil surface after the first rainstorm. However, the main factors were the greater rainfall energy delivered to the soil surface per minute (50% increase) and the increased amount and shear forces of the runoff caused by the higher rainfall intensity. Both factors increased the rate of soil detachment in the second rainstorm as compared with the first rainstorm, while the runoff had a higher transport capacity (Ferreira

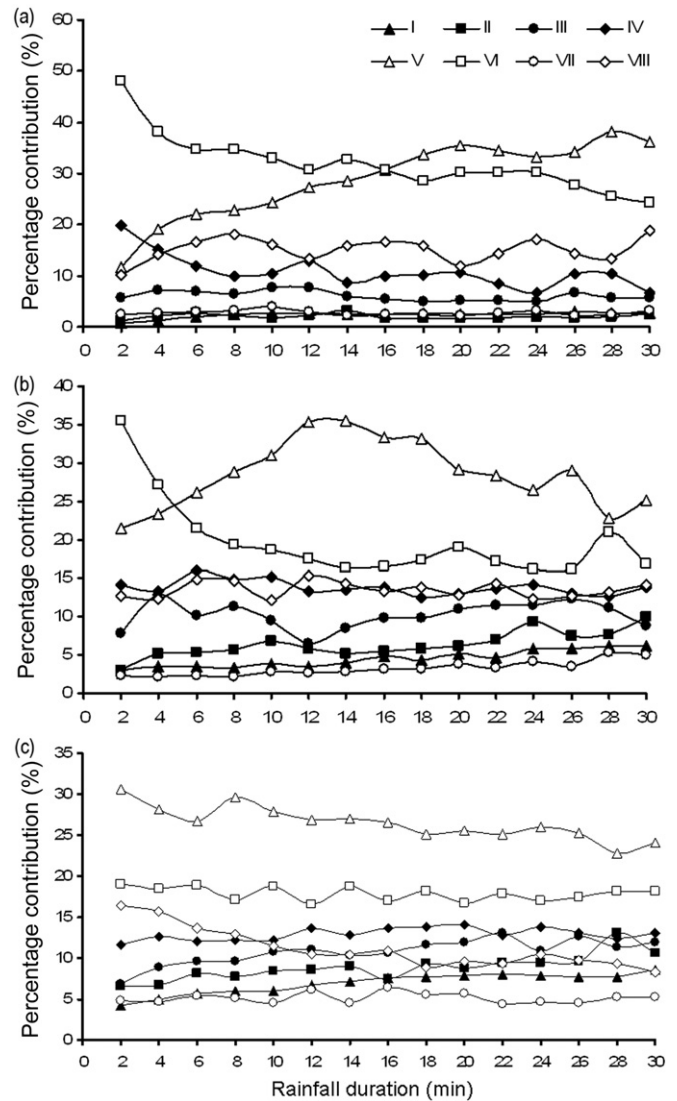


Fig. 4. Percentage contribution of each Region (REE I to VIII) to the total soil loss from the miniature watershed as a function of rainfall duration under three successive rainfalls with different intensities: (a) 1.0 mm min^{-1} , (b) 1.5 mm min^{-1} , and (c) 2.0 mm min^{-1} . I, upstream upper slopes; II, upstream lower slopes; III, downstream upper slopes; IV, downstream lower slopes; V, upper main gully; VI, lower main gully; VII, upper branch gullies; VIII, lower branch gullies.

and Singer, 1985; Mamedov et al., 2000). Fig. 4b shows that the contributions to the total soil loss from the watershed of the lower main gully (REE VI) decreased sharply from 35% to 20% in the first 6 min of the rainstorm and then fluctuated around a mean value of about 20%. In contrast, the contributions from the upper main gully (REE V) increased from 20% to 35% during the first half of the rainstorm and then decreased gradually during the second half. This indicated that the lower main gully developed faster and achieved stability earlier than the upper main gully. This can be ascribed to the greater erosivity of the runoff flowing in the lower main gully than that of the runoff flowing in the upper main gully, since the former commenced earlier and in greater amounts at higher flow rates, having received run-on water from the upper gully. As we observed, formation of rills, which dramatically increase soil loss (Lei et al., 2006; Liu et al., 2011b), continually developed on the slopes and on the branch gully side slopes, thereby increasing the contributions from these areas.

During the third and most intense rainstorm, the soil losses from every landform type exhibited relatively strong fluctuations during the first half of the rainstorm, while during the second half of the

rainstorm the fluctuations were notably less (Fig. 3c). Due to sandy soil with a very low cohesion and poor ability to resist erosion, the discontinuous and more abrupt collapsing of gully banks and growth of rills led to the strong fluctuations in soil losses. As the rainstorm progressed, the reduced availability of highly erodible sediment caused decreasing of soil loss. The contributions of gullies to total soil loss from REE V (upper main gully) and VIII (lower branch gullies) region gradually decreased from 31% and 16% to 23% and 8%, respectively (Fig. 4c). Only slight changes in the contributions from the other landform types were observed.

3.3. Soil loss from the slopes and gully system

Fig. 5 shows the contributions of the grouped sediment sources to the total soil loss of the watershed over the course of the three rainstorms. Soil loss from the gully system, comprising the main and branch gullies, was much greater than from the slopes, especially during the first rainstorm where soil loss from the gully system was 78.8% of total soil loss from the watershed while, correspondingly, from the slopes it was 21.2% (Table 2). During the second rainstorm, the contribution to soil loss by the gully system was 68.4% less than in the first rainstorm, while the contribution made by the slopes was greater (31.6%) (Table 2). In the third rainstorm, the contribution to soil loss from the gully system continued to decrease to 64.7%, while that of the slopes increased to 35.3% (Table 2).

Overall, soil loss from the watershed was mainly due to gully erosion for two main reasons. First, the gradients on the hill slopes were less than 10° , whereas those of the sideslopes and beds of the gullies were steeper, especially those of the sideslopes that were greater than 20° . If the gradient of a slope is greater than a critical value, then the slope is considered to be steep and soil loss is enhanced (Pan and Shangguan, 2006; Liu et al., 2010). Second, the amount and velocity of the runoff in the gullies was much greater than that on the hill slope and occurred as a concentrated flow rather than as sheet flow, thereby leading to greater soil losses (Nogueras et al., 2000; Poesen et al., 2003). The contribution to soil loss from the gully system decreased with each rain event while that from the slopes increased. During the second more intense rainstorm, rills developed that had been initiated on the slopes at the end of the first rainstorm. These rills continued to develop and increased the erosion. During the second and third rainstorms, the rills on the slopes continued to develop; the increases in rainfall intensity further accelerated the development of the rills, leading to higher soil losses from the slopes (Römkens et al., 2002). Although the amount of soil erosion increased from both the slopes and gully system, the rate of increase was faster for the slopes than for the gully system partly because the slopes account for a larger area

and partly because of the most readily available sediment having already been mobilized in the gully system.

The contributions to the total soil loss from the entire watershed from the main and branch gullies were different in the gully system. The contributions from the branch gullies stabilized at between 12% and 21%. However, the contribution was greater than 40%, and as high as 65%, from the main gully. Intense soil erosion was due to the concentrated flow in the main gully (Nogueras et al., 2000; Poesen et al., 2003).

An obvious difference in soil erosion from the upper and lower slopes was observed. The contribution to soil loss from the lower slope was greater than that from the upper slope during all three rainfall events. However, the difference between the two slope areas decreased with the increase in rainfall intensity and with the rainfall duration. This was attributed to the way in which rills were formed. The first occurrence of rill formation was on the lower slopes early in the rainstorm sequence. Then the rill-head migrated upslope. Thus, soil loss from the upper slopes increased when the rills reached the upper hillslope areas.

3.4. Analysis of the experimental error

The experimental errors in the three rainstorms were 35%, 25%, and 18% (Table 3). These errors were calculated using Eq. (3), and they represented over-estimations of erosion. Although the errors found in this study were greater than those found by studies in loess areas in China ($<15\%$) where the soil texture is finer (Liu et al., 2004; Lei et al., 2006), REEs still have the potential to be used as tracers to monitor soil erosion in areas with purple soils. However, the accuracy of this tracing method should be improved prior to application to field research or in studies where the soil texture is coarse.

Two potential sources of error exist in this study. First, the error could have been due to the calculation method we employed. The method employed in this study did not consider the selectivity of particles comprising the eroded sediments in the calculation of the contributions to total soil loss from the different areas. Fig. 6 provides a comparison of the particle size distribution of the parent material and that of all of the collected sediment samples. The particle size distribution is shown in the figure as a range of distributions denoted by the shaded area. The figure indicates that the particle size distribution of the collected eroded sediments was different from that of the parent material. For a given particle size less than 2 mm, the cumulative volumetric content of the sediment was larger than that of the parent soil. The most relevant finding is that the cumulative volumetric content of particles smaller than 0.5 mm in the sediment was approximately 10% larger than in the parent soil in all three rainstorms. These particles can absorb larger amounts of REEs (Mahler et al., 1998; Zhang et al., 2001; Kimoto et al., 2006b). Therefore, the calculated value of the eroded sediment would be overestimated if the selectivity of particles during the erosion processes was not considered. Data in Table 2 suggest the same conclusion. The error from the calculation method would be greater when applied over larger scales where the particle size selectivity during sediment mobilization might also be greater (Slattery and Burt, 1997; Walling et al., 2000; Amptouah et al., 2006). Second, the systemic and random error primarily from experimental instrument and operation could be existing. It should be pointed out that, over a larger scale, the errors mentioned here would probably be greater for practical reasons.

3.5. Applications

Runoff and erosion processes are affected by many factors such as soil, topography, precipitation, climate characteristics, land uses, conservation measures, etc. (Shi et al., 2004, 2012a; Fang et al., 2012). It is practically impossible to consider all of them simultaneously in a simulated experiment. In this study, only three factors, i.e., topography, precipitation, and soil properties were selected for study, since they

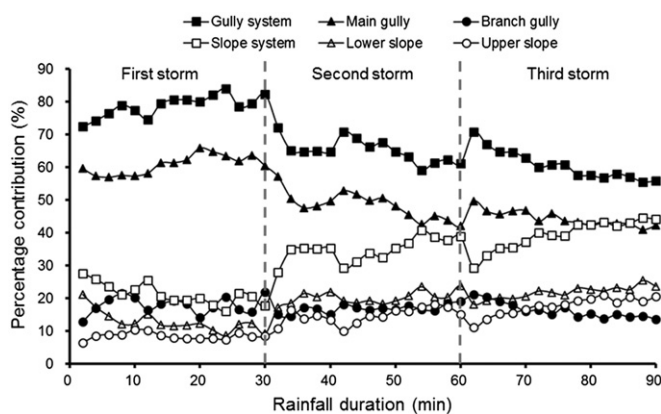


Fig. 5. Percentage contribution to the total soil loss from the miniature watershed of the slope and gully systems and their components as a function of rainfall duration under three successive 30-min-rainstorms with different intensities: 0–30 min at 1.0 mm min^{-1} , 30–60 min at 1.5 mm min^{-1} , 60–90 min at 2.0 mm min^{-1} .

Table 2
Amount and relative proportion of soil loss from different landform types.

Rare earth element oxides		La ₂ O ₃	Yb ₂ O ₃	CeO ₂	Sm ₂ O ₃	Eu ₂ O ₃	Tb ₄ O ₇	Nd ₂ O ₃	Ho ₂ O ₃
REE number		I	II	III	IV	V	VI	VII	VIII
Landform type		Upstream upper slopes	Upstream lower slopes	Downstream upper slopes	Downstream lower slopes	Upper main gully	Lower main gully	Upper branch gullies	Lower branch gullies
Rainfall intensity 1.0 (mm min ⁻¹)	Soil loss (kg)	0.140	0.117	0.326	0.549	1.598	1.633	0.156	0.809
	Relative soil loss (%) ^a	2.6	2.2	6.1	10.3	30.0	30.6	2.9	15.2
Rainfall intensity 1.5 (mm min ⁻¹)	Soil loss (kg)	1.356	3.152	0.981	4.289	8.925	6.125	4.233	1.959
	Relative soil loss (%) ^a	4.4	10.2	3.2	13.8	28.8	19.7	13.6	6.3
Rainfall intensity 2.0 (mm min ⁻¹)	Soil loss (kg)	2.136	3.349	1.598	4.03	8.332	5.633	3.533	2.756
	Relative soil loss (%) ^a	6.8	10.7	5.1	12.8	26.6	18.0	11.3	8.8

^a Relative soil loss is expressed as percent of total soil loss.

have greater effects on runoff and erosion processes and are easier to simulate than other factors. As a result, the characteristics of runoff and erosion processes in the experiment were very similar to those in a natural watershed from certain points of view. First, the Wangjiaqiao watershed included the small watershed that the miniature watershed modeled. For the watershed, the gully system made a greater contribution to sediments and had a higher transport capacity than the hill slope areas, and the erosion of gully side slopes, especially in the main gully, was a major source of sediment (Shi et al., 2004; Fang et al., 2011). These results were also observed in our study. Secondly, the selective transport of fine sediment and selective deposition of coarse sediment occurred mainly on the steep slopes (Shi et al., 2012a,b,c). Fig. 6 shows that the particle size distributions of the collected eroded sediments were all finer than that of the parent material, so selective transport of fine sediment also occurred in the miniature watershed. Furthermore, size selectivity may also occur among water stable aggregate sizes, especially when aggregate sizes are associated with selective particle size distributions (Kimoto et al., 2006b). Finally, data from the Wangjiaqiao watershed exhibited significant correlations among total precipitation, runoff, and suspended sediment (Fang et al., 2011). Fig. 2 and Table 3 indicate similar relationships among these variables in the miniature watershed. Furthermore, a small number of extreme rainfall events were observed to produce a large proportion of runoff and sediment in the natural watershed (Fang et al., 2011, 2013). Based on the natural maximum rainfall intensity occurring for a 30-min period, the simulated rainfall intensities of 1.5 and 2.0 mm min⁻¹ could be considered to represent such extreme natural rainfall events, and resulted in greater amounts of runoff and sediment in the miniature watershed than under the less extreme 1.0 mm min⁻¹ intensity.

However, differences also existed between the runoff and erosion processes of the miniature and natural watersheds. For example, flood discharge processes were more complicated at the larger scale than at the smaller scale. Three kinds of hysteretic loops were observed in the Wangjiaqiao watershed, i.e., clockwise, figure eight shapes, and complex hysteresis loops (Fang et al., 2011). Such hysteretic loops were not observed in the miniature watershed. This is caused not only by the difference between the scales, but also by the climate characteristics, land uses, and conservation measures that could not be easily simulated.

Table 3
Actual and calculated soil losses and experimental error for the three simulated rainstorm intensities.

Parameters	Rainfall intensity		
	1.0 (mm min ⁻¹)	1.5 (mm min ⁻¹)	2.0 (mm min ⁻¹)
Actual soil loss (kg)	3.937	24.789	26.579
Calculated soil loss (kg)	5.328	31.020	31.367
Error (%) ^a	35	25	18

^a The experimental error estimated used this equation: $\sigma = \left(\frac{W}{W} - 1\right) \times 100\%$. Where W is the calculated soil loss (kg); W is the actual soil loss.

Although more detailed or quantitative information about the interactions and feedbacks among the runoff and erosion processes could not be derived in this study, REEs could be used as a reasonably accurate tool by which eroded materials in the different landform types could be distinguished. Considering the spatial and temporal complexity of the runoff and erosion processes in a natural watershed, the REEs tracing method should be modified for application to the field. For example, applying the REEs as a point source or in sections based on the landform type should be done to reduce costs (Liu et al., 1997). Automated sampling systems within the natural watershed could be employed to provide detailed information about flooding, sediment transport, and deposition in real time during rainstorms. To improve the accuracy, soil type, which has an effect on particle size distributions in the sediments, must be considered when this methodology is adopted because one of the assumptions made in the calculations is that the particle size distributions of the source and sediment material are similar. Therefore, this method has the potential to be applied to landscape units with similar features (e.g., a small agricultural watershed) in order to monitor the sediment sources and erosion processes in different regions. However, if a good balance could be maintained between the costs and accuracy, a more applicable REEs tracing method for natural watersheds might also be developed in order to provide detailed information on the within-watershed patterns of erosion and deposition, which presently remain unclear.

4. Conclusions

Eight kinds of REE oxides were applied to a miniature watershed model. The model was established based on a field survey of a small watershed located in the Three Gorges area of China in order to estimate the proportions of sediments from eight different source positions. The concentration of REEs in the collected eroded material was analyzed to investigate soil erosion during three simulated rainfall events with intensities of 1.0, 1.5, and 2.0 mm min⁻¹.

During the three rainfall events, the erosion fluctuated relative to landform type. For example, the percentage contribution to the total soil loss from the entire watershed by the lower main gully (REE VI) initially decreased and then stabilized under a rainfall intensity of 1.5 mm min⁻¹, whereas that from the upper main gully (REE V) initially increased and then decreased. Contributions from the other landform types increased steadily and then stabilized. Overall, the contributions from the gully system were greater than those from the hill slopes. Contributions from the gully system tended to decrease as rainfall intensity and duration of the rainstorm increased, whereas those from the hill slopes tended to increase. Contributions from the lower hill slopes were greater than those from the upper hill slopes but the differences decreased as the rainfall intensity and duration of rainfall increased.

We concluded that, in general, the use of REEs to study the source areas of soil erosion at different positions in a miniature watershed with purple soils during rainfall events could be reasonably accurate

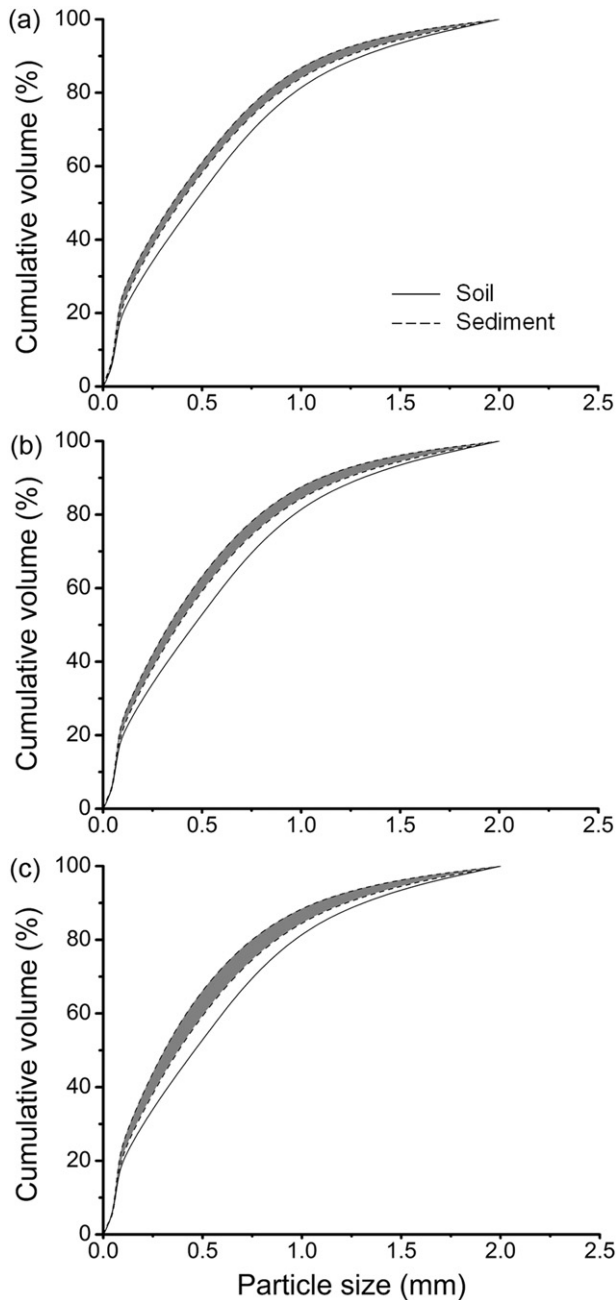


Fig. 6. Particle size distributions (PSD) of the parent soil and of the various suspended sediments. The shaded area is the range of PSDs of the suspended sediments discharged from the miniature watershed during three successive rainstorms of different intensity: (a) 1.0 mm min^{-1} , (b) 1.5 mm min^{-1} , and (c) 2.0 mm min^{-1} .

and advantageous. Based on the observed soil losses in this study, REEs should be added to soils to greater depths in gully areas where concentrated flow and bank collapses result in erosion to greater depths as compared with hill slope areas where sheet flow occurs and only a thin layer of soil is removed. Integrating the use of REEs as tracers, monitoring of sediments, rainfall simulation, and *in situ* measurements is an effective method of studying erosion processes in relation to landform features. However, more research is required prior to the application of the approach to large natural watersheds. In particular, the calculation method requires improvement due to its unrealistic assumption that the particle size distributions of the parent soil and sediments are the same. Understanding the sources of soil erosion is important not only in building process-driven mathematical models that accurately predict soil loss at various temporal and spatial scales but also in

evaluating the effectiveness of management methods implemented to conserve soil.

Acknowledgment

We thank editors and anonymous reviewers for their valuable comments on the manuscript, and thank Dr. Glenn Wilson for his suggestions and improving the English writing of the manuscript. This research was jointly supported by the National Key Technology Research and Development Program of the Ministry of Science and Technology of China (No. 2015BAC01B03-03), the National Natural Science Foundation of China (No. 41201270), the West Light Foundation of the Chinese Academy of Sciences (No. 2014-91), the Shaanxi Science and Technology Co-ordination Innovation Engineering Project (No. 2013KTDZ03-03-01), the Scientific Research Foundation of Northwest A&F University (No. 2013BSJJ082), the Talents Research Start-up Foundation of Shaanxi Province (No. 2013-02100-Z111021512), and the China Scholarship Council (No. 201404910141).

References

- Agassi, M., Shainberg, I., Morin, J., 1981. Effect of electrolyte concentration and soil sodicity on infiltration rate and crust formation. *Soil Sci. Soc. Am. J.* 45, 848–851.
- Amptuah, E.O., Robinson, J.S., Nortcliff, S., 2006. Assessment of soil particle redistribution on two contrasting cultivated hillslopes. *Geoderma* 132, 324–343.
- Anonymous, 2004. Soil and trouble. *Science* 304, 1614–1615.
- Fang, N.F., Shi, Z.H., Li, L., Jiang, C., 2011. Rainfall, runoff, and suspended sediment delivery relationships in a small agricultural watershed of the Three Gorges area, China. *Geomorphology* 135, 158–166.
- Fang, N.F., Shi, Z.H., Li, L., Guo, Z.L., Liu, Q.J., Ai, L., 2012. The effects of rainfall regimes and land use changes on runoff and soil loss in a small mountainous watershed. *Catena* 99, 1–8.
- Fang, N.F., Shi, Z.H., Yue, B.J., Wang, L., 2013. The characteristics of extreme erosion events in a small mountainous watershed. *PLoS One* 8, 1–10.
- Ferreira, A.G., Singer, M.J., 1985. Energy dissipation for water drop impact into shallow pools. *Soil Sci. Soc. Am. J.* 49, 1537–1542.
- Greenwood, P., 2012. Tracing fine-sediment using artificial radionuclides. In: Clarke, L.E., Nield, J.M. (Eds.), *Geomorphological Techniques*, Chapter 3, Section 5.2. British Society for Geomorphology, London, UK, pp. 1–10.
- Greenwood, P., Walling, D.E., Quine, T.A., 2014. Using caesium-134 and cobalt-60 as tracers to assess the remobilization of recently-deposited overbank-derived sediment on river floodplains during subsequent inundation events. *Earth Surf. Process. Landf.* 39, 228–244.
- Kimoto, A., Nearing, M.A., Shipitalo, M.J., Polyakov, V.O., 2006a. Multi-year tracking of sediment sources in a small agricultural watershed using rare earth elements. *Earth Surf. Process. Landf.* 31, 1763–1774.
- Kimoto, A., Nearing, M.A., Zhang, X.C., Powell, D.M., 2006b. Applicability of rare earth element oxides as a sediment tracer for coarse-textured soils. *Catena* 65, 214–221.
- Lei, T.W., Zhang, Q.W., Zhao, J., Nearing, M.A., 2006. Tracing sediment dynamics and sources in eroding rills with rare earth elements. *Eur. J. Soil Sci.* 57, 287–294.
- Li, M., Li, Z.B., Ding, W.F., Liu, P.L., Yao, W.Y., 2006. Using rare earth element tracers and neutron activation analysis to study rill erosion process. *Appl. Radiat. Isot.* 64, 402–408.
- Liu, P.L., Tian, J.L., Zhou, P.H., Li, Y.Q., Ju, T.J., 1997. Studies of operating techniques on REE tracer method applying to soil erosion. *Res. Soil Water Conserv.* 4, 10–16.
- Liu, P.L., Tian, J.L., Zhou, P.H., Yang, M.Y., Shi, H., 2004. Stable rare earth element tracers to evaluate soil erosion. *Soil Tillage Res.* 76, 147–155.
- Liu, G., Tian, F.X., Warrington, D.N., Zheng, S.Q., Zhang, Q., 2010. Efficacy of grass for mitigating runoff and erosion from an artificial loessial earthen road. *Trans. ASABE* 53, 119–125.
- Liu, G., Liu, P.L., Warrington, D.N., Ju, T.J., Zhang, Q., Xu, W.N., 2011a. Resolving ecological and economic challenges: an application of sustainable ecological agriculture on the Chinese Loess Plateau. *J. Food Agric. Environ.* 9, 575–582.
- Liu, G., Yang, M.Y., Warrington, D.N., Liu, P.L., Tian, J.L., 2011b. Using beryllium-7 to monitor the relative proportions of interrill and rill erosion from loessial soil slopes in a single rainfall event. *Earth Surf. Process. Landf.* 36, 439–448.
- Lu, X.X., Higgitt, D.L., 1998. Recent changes of sediment yield in the upper Yangtze, China. *Environ. Manag.* 22, 697–709.
- Lu, X.X., Ashmore, P., Wang, J., 2003. Sediment load mapping in a large river basin: the upper Yangtze, China. *Environ. Model. Softw.* 18, 339–353.
- Mahler, B.J., Bennett, P.C., Zimmerman, M., 1998. Lanthanide-labeled clay: a new method for tracing sediment transport in Karst. *Groundwater* 36, 835–843.
- Mamedov, A.I., Shainberg, I., Levy, G.J., 2000. Rainfall energy effects on runoff and interrill erosion in effluent irrigated soils. *Soil Sci.* 165, 535–544.
- Matisoff, G., Ketterer, M.E., Wilson, C.G., Layman, R., Whiting, P.J., 2001. Transport of rare earth element-tagged soil particles in response to thunderstorm runoff. *Environ. Sci. Technol.* 35, 3356–3362.
- Michaelides, K., Ibrahim, I., Nord, G., Esteves, M., 2010. Tracing sediment redistribution across a break in slope using rare earth elements. *Earth Surf. Process. Landf.* 35, 575–587.

- Moore, D.C., Singer, M.J., 1990. Crust formation effects on soil erosion processes. *Soil Sci. Soc. Am. J.* 54, 1117–1123.
- Noguera, P., Burjachs, F., Gallart, F., Puigdefàbregas, J., 2000. Recent gully erosion in the El Cautivo badlands (Tabernas, SE Spain). *Catena* 40, 203–215.
- Olmez, I., Pink, F.X., Wheatcroft, R.A., 1994. New particle-labeling technique for use in biological and physical sediment transport studies. *Environ. Sci. Technol.* 28, 1487–1490.
- Pan, C.Z., Shangguan, Z.P., 2006. Runoff hydraulic characteristics and sediment generation in sloped grassplots under simulated rainfall conditions. *J. Hydrol.* 331, 178–185.
- Poesen, J., Nachtergaele, J., Verstraeten, G., Valentin, C., 2003. Gully erosion and environmental change: importance and research needs. *Catena* 50, 91–133.
- Polyakov, V.O., Nearing, M.A., 2004. Rare earth element oxides for tracing sediment movement. *Catena* 55, 255–276.
- Polyakov, V.O., Nearing, M.A., Shipitalo, M.J., 2004. Tracking sediment redistribution in a small watershed: implications for agro-landscape evolution. *Earth Surf. Process. Landf.* 29, 1275–1291.
- Polyakov, V.O., Kimoto, A., Nearing, M.A., Nichols, M.H., 2009. Tracing sediment movement on a semiarid watershed using rare earth elements. *Soil Sci. Soc. Am. J.* 73, 1559–1565.
- Römkens, M.J.M., Helming, K., Prasad, S.N., 2002. Soil erosion under different rainfall intensities, surface roughness, and soil water regimes. *Catena* 46, 103–123.
- Shi, H., Shao, M.A., 2000. Soil and water loss from the Loess Plateau in China. *J. Arid Environ.* 45, 9–20.
- Shi, H., Tian, J.L., Liu, P.L., Zhou, P.H., 1997. A study on sediment sources in a small watershed by using REE tracer method. *Sci. China (Ser. E)* 40, 12–20.
- Shi, Z.H., Cai, C.F., Ding, S.W., Wang, T.W., Chow, T.L., 2004. Soil conservation planning at the small watershed level using RUSLE with GIS: a case study in the Three Gorge Area of China. *Catena* 55, 33–48.
- Shi, Z.H., Chen, L.D., Cai, C.F., Li, Z.X., Liu, G.H., 2009. Effects of long-term fertilization and mulch on soil fertility in contour hedgerow systems: a case study on steeplands from the Three Gorges Area, China. *Nutr. Cycl. Agroecosyst.* 84, 39–48.
- Shi, Z.H., Ai, L., Fang, N.F., Zhu, H.D., 2012a. Modeling the impacts of integrated small watershed management on soil erosion and sediment delivery: a case study in the Three Gorges Area, China. *J. Hydrol.* 438–439, 156–167.
- Shi, Z.H., Fang, N.F., Wu, F.Z., Wang, L., Yue, B.J., Wu, G.L., 2012b. Soil erosion processes and sediment sorting associated with transport mechanisms. *J. Hydrol.* 454–455, 123–130.
- Shi, Z.H., Yue, B.J., Wang, L., Fang, N.F., Wang, D., Wu, F.Z., 2012c. Effects of mulch cover rate on interrill erosion processes and the size selectivity of eroded sediment on steep slopes. *Soil Sci. Soc. Am. J.* 77, 257–267.
- Slattery, M.C., Burt, T.P., 1997. Particle size characteristics of suspended sediment in hillslope runoff and stream flow. *Earth Surf. Process. Landf.* 22, 705–719.
- Soil Survey Staff, 1999. *Soil Taxonomy: A Basic System of Soil Classification for Making and Interpreting Soil Surveys*. US Dep. Agric. Handbook vol. 436 pp. 489–554 (Washington, DC).
- Stevens, C.J., Quinton, J.N., 2008. Investigating source areas of eroded sediments transported in concentrated overland flow using rare earth element tracers. *Catena* 74, 31–36.
- Tian, J.L., Zhou, P.H., Liu, P.L., 1994. REE tracer method for studies on soil erosion. *Int. J. Sediment Res.* 9, 39–46.
- US EPA, 1995. *Test Methods for Evaluating Solid Waste (SW 846)*. third ed. US Government Printing Office, Washington, DC.
- Ventura, E., Nearing, M.A., Norton, L.D., 2001. Developing a magnetic tracer to study soil erosion. *Catena* 43, 277–291.
- Wallbrink, P.J., Martin, C.E., Wilson, C.J., 2003. Quantifying the contributions of sediment, sediment-P and fertiliser-P from forested, cultivated and pasture areas at the landuse and catchment scale using fallout radionuclides and geochemistry. *Soil Tillage Res.* 69, 53–68.
- Walling, D.E., He, Q., 1997. Use of fallout ¹³⁷Cs in investigations of overbank sediment deposition on river floodplains. *Catena* 29, 263–282.
- Walling, D.E., Owens, P.N., Waterfall, B.D., Leeks, G.J.L., Wass, P.D., 2000. The particle size characteristics of fluvial suspended sediment in the Humber and Tweed catchments, UK. *Sci. Total Environ.* 251–252, 205–222.
- Williams, J.D., Wilkins, D.E., McCool, D.K., Baarstad, L.L., Klepper, B.L., Papendick, R.I., 1998. A new rainfall simulator for use in low-energy rainfall areas. *Appl. Eng. Agric.* 14, 243–247.
- Wooldridge, D.D., 1965. Tracing soil particle movement with Fe-59. *Soil Sci. Soc. Am. J.* 29, 469–472.
- Yang, W.D., Wang, Z.Q., Sui, G.P., Ding, G.W., 2008. Quantitative determination of red-soil erosion by an Eu tracer method. *Soil Tillage Res.* 101, 52–56.
- Young, R.A., Holt, R.F., 1968. Tracing soil movement with fluorescent glass particles. *Soil Sci. Soc. Am. J.* 32, 600–602.
- Zhang, X.C., Friedrich, J.M., Nearing, M.A., Norton, L.D., 2001. Potential use of rare earth oxides as tracers for soil erosion and aggregation studies. *Soil Sci. Soc. Am. J.* 65, 1508–1515.
- Zhang, X.C., Nearing, M.A., Polyakov, V.O., Friedrich, J.M., 2003. Using rare-earth oxide tracers for studying soil erosion dynamics. *Soil Sci. Soc. Am. J.* 67, 279–288.